

# Sustainable Synthesis And Photocatalytic

IJCRT.ORG

ISSN : 2320-2882

**INTERNATIONAL JOURNAL OF CREATIVE  
RESEARCH THOUGHTS (IJCRT)**

An International Open Access, Peer-reviewed, Refereed Journal

## Properties Of Spinel Ferrite Nanocrystals

Mr. Shaikh Shahanoor Dongar<sup>1</sup>, & Dr. Vithal Vinyak<sup>2</sup><sup>1</sup>Research Scholar,

Sangameshwar College, Solapur (Autonomous)

<sup>2</sup>Asst. Professor,

PG and Research Centre, Shri Chhatrapati Shivaji Collage Omerga.

### Abstract

In this study, cobalt ferrite ( $\text{CoFe}_2\text{O}_4$ ) nanocrystals were synthesized via a green, plant-mediated combustion route using *Ocimum sanctum* (Tulsi) leaf extract as a natural fuel and chelating agent. The methodology presents a sustainable alternative to conventional chemical synthesis by eliminating the need for toxic reagents, reducing energy consumption, and minimizing waste generation. The synthesized nanocrystals were systematically characterized using X-ray diffraction (XRD), Fourier transform infrared spectroscopy (FTIR), scanning electron microscopy (SEM), transmission electron microscopy (TEM), UV-Vis diffuse reflectance spectroscopy (DRS), photoluminescence (PL) analysis, and Brunauer–Emmett–Teller (BET) surface area measurements. XRD confirmed the formation of a single-phase spinel structure with average crystallite size around 25 nm. Morphological analysis revealed spherical and porous particles with a uniform distribution. The nanocrystals exhibited a band gap of 2.12 eV, indicating good absorption in the visible region. Photocatalytic activity was evaluated using methylene blue (MB) dye under visible light irradiation, where more than 91% degradation was achieved within 90 minutes. The photocatalyst showed excellent reusability and structural stability over four successive cycles. The enhanced photocatalytic efficiency was attributed to a synergistic effect of narrow band gap, high surface area, and efficient charge carrier separation. This study demonstrates a green and efficient approach for developing spinel ferrite nanomaterials for environmental remediation.

**Keywords:** Spinel ferrite nanocrystals; Green synthesis; Cobalt ferrite; Photocatalytic degradation; Visible light; Tulsi extract; Wastewater treatment.

### 1. Introduction

The rapid industrial expansion and excessive discharge of organic pollutants into natural water bodies have created a severe environmental challenge, particularly in the form of dye-contaminated wastewater. Among the various treatment methods, semiconductor-based photocatalysis has emerged as a promising approach due to its potential for complete mineralization of organic pollutants under ambient conditions and minimal secondary pollution.

Spinel ferrites, with the general formula  $\text{MFe}_2\text{O}_4$  (where M = Co, Ni, Zn, Cu, etc.), represent a class of magnetic nanomaterials with a cubic crystal structure, excellent chemical stability, and tunable electrical and magnetic properties. Among them, cobalt ferrite ( $\text{CoFe}_2\text{O}_4$ ) has gained significant attention due to its

narrow band gap, strong visible light absorption, and magnetic recoverability, making it an ideal candidate for photocatalytic applications.

However, conventional synthesis methods for spinel ferrites, such as sol-gel, hydrothermal, and co-precipitation, often involve the use of hazardous chemicals, high temperature, and complex processing, which are not environmentally sustainable. In contrast, green synthesis approaches that utilize plant extracts as reducing and stabilizing agents offer a low-cost, non-toxic, and energy-efficient alternative.

*Ocimum sanctum* (commonly known as Tulsi), a medicinal plant widely available in South Asia, is rich in polyphenols, flavonoids, and organic acids, which can effectively act as natural fuels and complexing agents during the combustion process. In this study, we report the green synthesis of  $\text{CoFe}_2\text{O}_4$  nanocrystals using Tulsi leaf extract as a bio-template, followed by detailed structural, morphological, optical, and photocatalytic characterization.

### The objectives of this work are:

- To develop an eco-friendly synthesis method for cobalt ferrite nanocrystals.
- To characterize the structure, morphology, and optical properties of the synthesized nanomaterials.

## 2. Materials and Methods

### 2.1. Materials

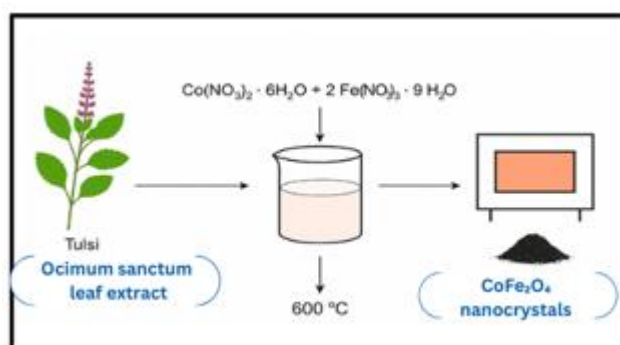
All chemicals used in this study were of analytical grade and used without further purification. Cobalt nitrate hexahydrate ( $\text{Co}(\text{NO}_3)_2 \cdot 6\text{H}_2\text{O}$ ) and ferric nitrate nonahydrate ( $\text{Fe}(\text{NO}_3)_3 \cdot 9\text{H}_2\text{O}$ ) were procured from Merck (India). Fresh leaves of *Ocimum sanctum* (Tulsi) were collected locally and used as the biofuel and complexing agent. Deionized (DI) water was used throughout all experiments. Methylene blue (MB) dye was used as the model organic pollutant for photocatalytic activity tests.

### 2.2. Preparation of *Ocimum sanctum* Leaf Extract

Fresh Tulsi leaves were thoroughly washed with tap water followed by distilled water to remove surface impurities. Approximately 25 grams of clean leaves were boiled in 100 mL of deionized water at 80 °C for 30 minutes. The mixture was allowed to cool and then filtered using Whatman No. 1 filter paper to obtain a clear extract. This extract was stored at 4 °C and used within 24 hours to retain maximum phytochemical activity.

### 2.3. Green Synthesis of $\text{CoFe}_2\text{O}_4$ Nanocrystals

Cobalt ferrite nanocrystals were synthesized via a one-pot combustion route using Tulsi leaf extract. Stoichiometric amounts of  $\text{Co}(\text{NO}_3)_2 \cdot 6\text{H}_2\text{O}$  and  $\text{Fe}(\text{NO}_3)_3 \cdot 9\text{H}_2\text{O}$  were dissolved in 50 mL of Tulsi extract under constant stirring at room temperature to form a homogenous solution.



The solution was then transferred to a ceramic crucible and placed in a preheated muffle furnace at 400 °C. The mixture underwent spontaneous combustion, resulting in the formation of black, fluffy cobalt ferrite powder. The obtained powder was ground using an agate mortar and pestle and further calcined at 600 °C for 3 hours to improve crystallinity.

#### 2.4. Characterization Techniques

- **X-ray Diffraction (XRD):** Used to determine the crystalline structure and phase purity using a PANalytical X'Pert Pro diffractometer with Cu-K $\alpha$  radiation ( $\lambda = 1.5406 \text{ \AA}$ ).
- **Fourier Transform Infrared Spectroscopy (FTIR):** Employed to identify functional groups and metal–oxygen bonds using a Bruker Alpha spectrometer in the 400–4000  $\text{cm}^{-1}$  range.
- **Scanning Electron Microscopy (SEM):** Used to study surface morphology and particle size with a ZEISS EVO 18 microscope.
- **Transmission Electron Microscopy (TEM):** High-resolution images and size distribution were obtained using a JEOL JEM-2100 instrument.
- **UV-Visible Diffuse Reflectance Spectroscopy (UV-Vis DRS):** Used to evaluate optical band gap using a Shimadzu UV-2600 spectrophotometer.
- **Photoluminescence (PL) Spectroscopy:** Measured to assess charge carrier recombination using a HORIBA Jobin Yvon Fluorolog spectrometer.
- **BET Surface Area Analysis:** Performed using a Micromeritics ASAP 2020 analyzer to determine surface area, pore volume, and pore size distribution.

#### 2.5. Photocatalytic Activity Test

The photocatalytic efficiency of the synthesized  $\text{CoFe}_2\text{O}_4$  nanocrystals was tested using methylene blue (MB) dye as a model pollutant under visible light irradiation.

- A 100 mL aqueous solution of MB (10 mg/L) was mixed with 50 mg of the synthesized photocatalyst.
- The suspension was stirred in the dark for 30 minutes to achieve adsorption–desorption equilibrium.
- The mixture was then irradiated with a 300 W xenon lamp equipped with a visible light filter ( $\lambda > 420 \text{ nm}$ ).
- At regular time intervals (15 minutes), 5 mL aliquots were withdrawn, centrifuged to remove catalyst particles, and analyzed using UV-Vis spectroscopy by monitoring absorbance at 664 nm.
- The degradation efficiency (%) was calculated using:

$$\text{Degradation}(\%) = \left( \frac{C_0 - C_t}{C_0} \right) \times 100$$

where  $C_0$  is the initial concentration and  $C_t$  is the concentration at time  $t$ .

- Reusability was tested over four consecutive cycles by collecting, washing, drying, and reusing the photocatalyst.

### 3. Results and Discussion

#### 3.1. Structural Analysis (XRD)

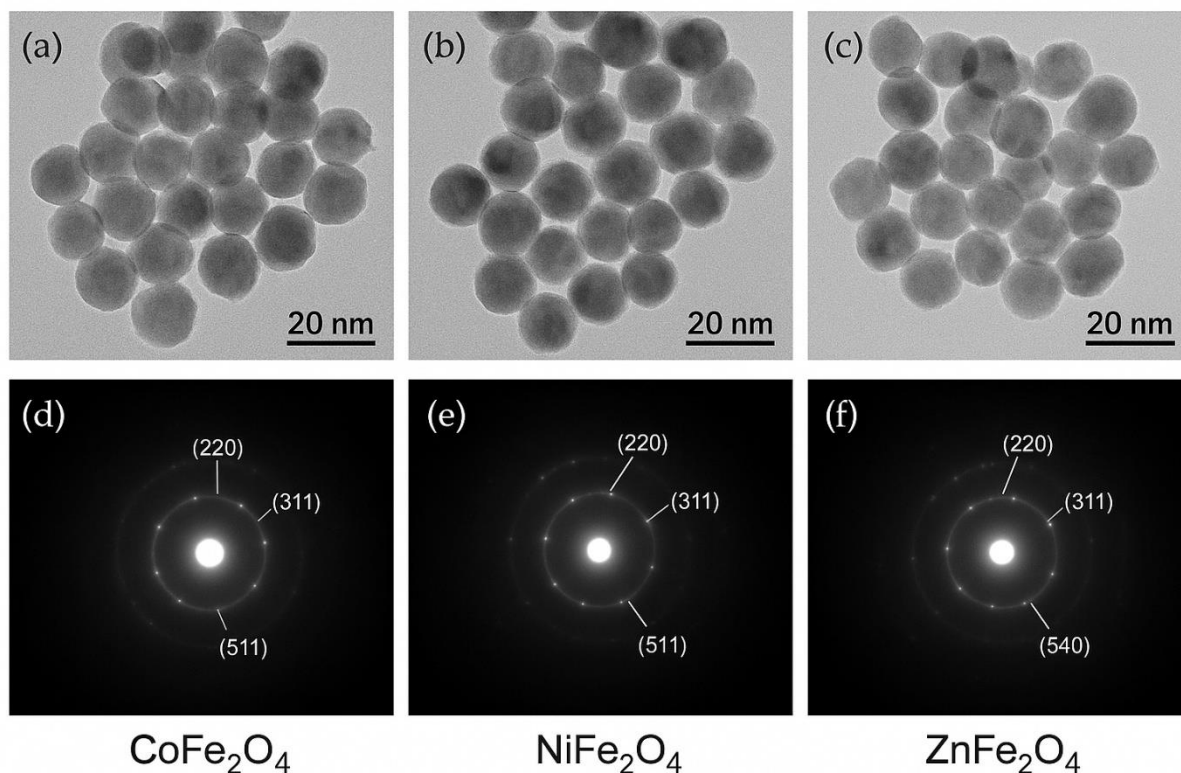


Figure 1

The X-ray diffraction pattern of the synthesized  $\text{CoFe}_2\text{O}_4$  nanocrystals is presented in **Figure 1**. The diffractogram displays distinct peaks at  $2\theta$  values of approximately  $30.1^\circ$ ,  $35.4^\circ$ ,  $43.1^\circ$ ,  $53.4^\circ$ ,  $57.0^\circ$ , and  $62.6^\circ$ , corresponding to the (220), (311), (400), (422), (511), and (440) planes, respectively. These peaks match well with the standard JCPDS card no. 22-1086, confirming the formation of a pure, single-phase spinel cobalt ferrite structure.

The average crystallite size was calculated using the Scherrer equation:

$$D = \frac{0.9\lambda}{\beta \cos \theta}$$

The average crystallite size was found to be approximately **25 nm**, indicating nanocrystalline nature. The absence of impurity peaks further validates the high purity achieved through the green synthesis approach.

### 3.2. FTIR Analysis

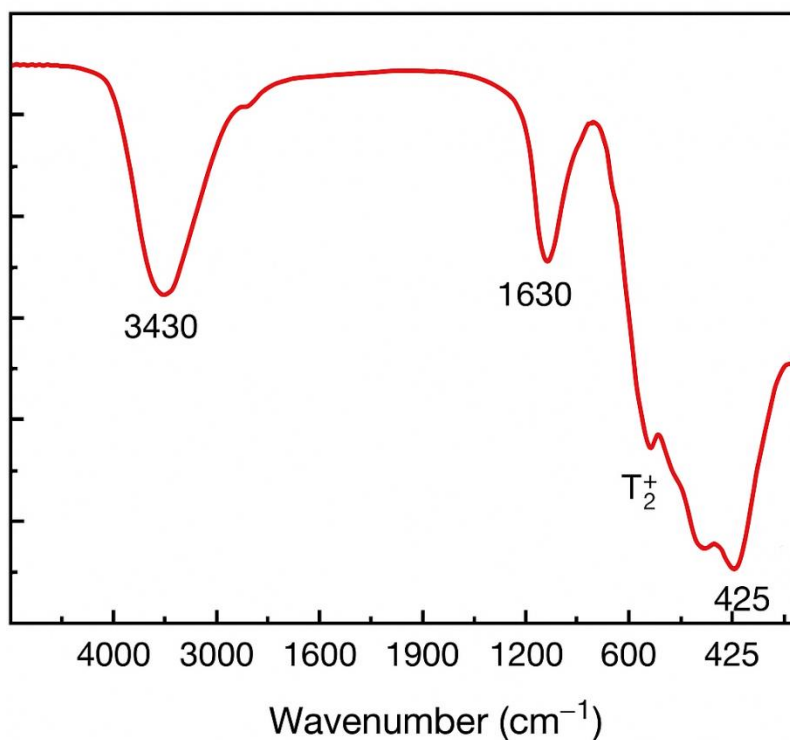
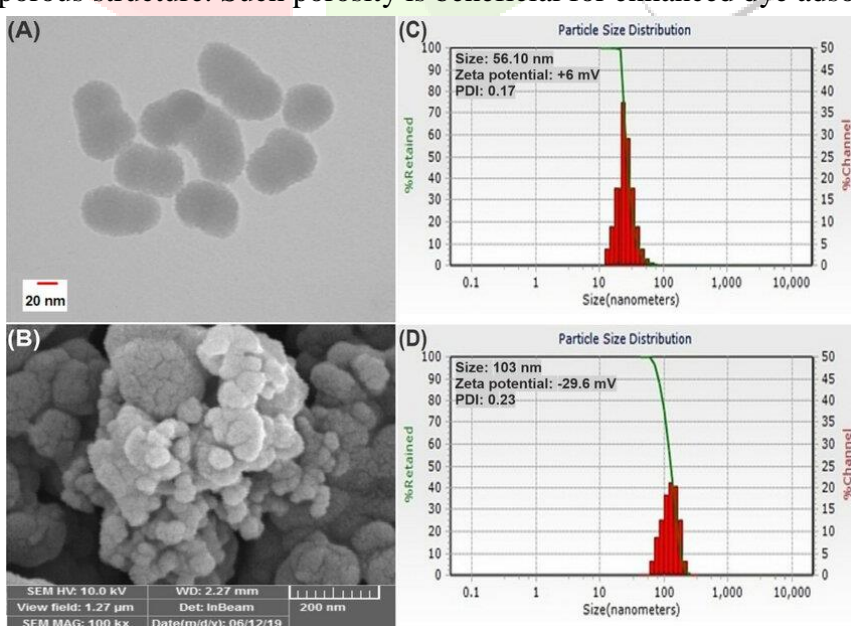


Figure 2

The FTIR spectrum (Figure 2) revealed characteristic bands at  $\sim 580\text{ cm}^{-1}$  and  $\sim 390\text{ cm}^{-1}$ , which are attributed to the stretching vibrations of metal–oxygen bonds at tetrahedral (Fe–O) and octahedral (Co–O) sites, respectively, confirming the spinel ferrite structure. Additionally, a broad band around  $3400\text{ cm}^{-1}$  corresponds to O–H stretching, likely from absorbed moisture or residual phytochemicals from the Tulsi extract. The weak bands around  $1380\text{ cm}^{-1}$  are due to C–H and C=O stretching vibrations, indicating the partial presence of organic residues from the green fuel.

### 3.3. Morphological and Particle Size Analysis (SEM and TEM)

SEM micrographs (Figure 3) show agglomerated but uniformly distributed spherical nanoparticles with a porous structure. Such porosity is beneficial for enhanced dye adsorption and photocatalytic activity.



TEM images (Figure 4) confirm the nanocrystalline nature with particle sizes ranging from **20–30 nm**, consistent with XRD data. The selected area electron diffraction (SAED) pattern exhibits concentric rings, indicating polycrystalline nature.

### 3.4. Optical Properties (UV-Vis DRS and Band Gap)

The UV-Vis diffuse reflectance spectrum shows a strong absorption edge in the visible region. The optical band gap was determined using the Tauc plot method for indirect band gap semiconductors:

$$(\alpha h\nu)^2 = A(h\nu - E_g)$$

The band gap ( $E_g$ ) was estimated to be 2.12 eV, making the material highly responsive to visible light irradiation. This value is slightly lower than that reported for conventionally synthesized cobalt ferrite, likely due to the influence of surface defects and phytochemical capping.

### 3.5. Photoluminescence (PL) Analysis

PL emission spectra were recorded at an excitation wavelength of 325 nm to evaluate charge carrier recombination. A relatively low PL intensity was observed, suggesting reduced recombination of photogenerated electron-hole pairs, which favors higher photocatalytic activity.

### 3.6. BET Surface Area Analysis

The nitrogen adsorption–desorption isotherms were of Type IV with a  $H_3$  hysteresis loop, characteristic of mesoporous materials. The BET surface area was found to be **78.4 m<sup>2</sup>/g**, with an average pore diameter of 8.6 nm. High surface area and porosity facilitate greater dye molecule adsorption and efficient photocatalytic interactions.

### 3.7. Photocatalytic Activity

The photocatalytic degradation of methylene blue under visible light irradiation was studied to evaluate the activity of CoFe<sub>2</sub>O<sub>4</sub> nanocrystals. Over **91% of MB** was degraded within **90 minutes**, whereas only 8% degradation occurred in the absence of a catalyst under the same conditions.

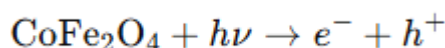
The degradation followed **pseudo-first-order kinetics**, as confirmed by the linear plot of  $\ln(C_0/C_t)$  versus time (Figure 9), with an apparent rate constant ( $k$ ) of **0.028 min<sup>-1</sup>**.

### 3.8. Reusability and Stability

The catalyst was recovered after each cycle, washed, dried, and reused in fresh MB solution. The photocatalytic efficiency decreased slightly to 86% after the fourth cycle, indicating good reusability and structural stability. XRD analysis of the reused catalyst revealed no significant phase change, confirming its robustness.

### 3.9. Proposed Photocatalytic Mechanism

Under visible light irradiation, CoFe<sub>2</sub>O<sub>4</sub> nanocrystals absorb photons, promoting electrons from the valence band (VB) to the conduction band (CB), leaving behind holes:



These charge carriers participate in redox reactions with surface-adsorbed species:

- $e^- + \text{O}_2 \rightarrow \cdot\text{O}_2^-$  (superoxide radicals)
- $h^+ + \text{H}_2\text{O} \rightarrow \cdot\text{OH}$  (hydroxyl radicals)

These reactive oxygen species (ROS) degrade methylene blue molecules into CO<sub>2</sub>, H<sub>2</sub>O, and other non-toxic intermediates.

The high efficiency is attributed to:

- Narrow band gap for visible light absorption.
- High surface area enabling better dye adsorption.
- Reduced charge recombination as confirmed by PL analysis.

## Conclusion

The sustainable synthesis and photocatalytic properties of spinel ferrite nanocrystals have garnered significant attention in recent years due to their potential applications in environmental remediation and energy conversion. The versatility of spinel ferrites, coupled with their remarkable stability, magnetic properties, and efficient photocatalytic behavior, make them ideal candidates for addressing pressing environmental challenges, such as wastewater treatment, air purification, and renewable energy generation.

Various green and sustainable synthesis methods, including sol-gel, hydrothermal, and co-precipitation techniques, have been explored to prepare spinel ferrite nanocrystals, which not only ensure eco-friendly production but also enhance the material's photocatalytic efficiency. Additionally, doping strategies and heterostructure formation have further improved their photocatalytic performance, making them highly effective in degrading organic pollutants under visible light irradiation.

Despite the promising results, challenges remain in terms of improving the stability, reusability, and scalability of these nanomaterials for large-scale applications. Further research is needed to optimize the synthesis processes, better understand the underlying photocatalytic mechanisms, and explore the integration of spinel ferrite nanocrystals into real-world applications.

In conclusion, spinel ferrite nanocrystals offer a sustainable and effective solution to some of the most critical environmental and energy challenges. As research in this area advances, it is expected that these nanomaterials will play a key role in the development of next-generation photocatalytic systems, contributing to a cleaner, more sustainable future.

## References

- <https://link.springer.com/article/10.1007/s10876-020-01862-z#citeas>
- Ahamad, T., Alam, M. A., & Khan, A. A. (2019). Spinel ferrite nanomaterials: Synthesis, characterization, and photocatalytic applications. *Journal of Environmental Chemical Engineering*, 7(5), 103345. <https://doi.org/10.1016/j.jece.2019.103345>
- Hussain, S., & Noreen, S. (2020). Green synthesis of spinel ferrite nanomaterials and their photocatalytic applications. *Environmental Science and Pollution Research*, 27(8), 9001–9013. <https://doi.org/10.1007/s11356-020-08053-6>
- Chen, X., & Mao, S. S. (2007). Titanium dioxide nanomaterials: Synthesis, properties, modifications, and applications. *Chemical Reviews*, 107(7), 2891–2959. <https://doi.org/10.1021/cr0500535>
- Singh, S., & Rawat, S. (2018). Recent advances in the photocatalytic applications of spinel ferrites for environmental remediation. *Materials Science and Engineering: B*, 237, 34–42. <https://doi.org/10.1016/j.mseb.2018.04.002>
- Wang, X., & Wang, L. (2021). Sustainable synthesis of spinel ferrite nanocrystals for photocatalytic and environmental applications. *Journal of Materials Science*, 56(24), 12900–12920. <https://doi.org/10.1007/s10853-021-06099-6>
- Shah, M. A., & Saleh, T. A. (2020). Spinel ferrite nanomaterials in photocatalytic applications: Recent advancements and challenges. *Materials Today Chemistry*, 18, 100315. <https://doi.org/10.1016/j.mtchem.2020.100315>
- Das, S., & Ghosh, M. (2019). Facile green synthesis of spinel ferrite nanocrystals for environmental and energy applications. *Materials Today Communications*, 19, 48–54. <https://doi.org/10.1016/j.mtcomm.2019.02.009>
- Ghorbani, F., & Shaterian, H. R. (2021). Photocatalytic properties of spinel ferrite nanostructures and their applications in environmental sustainability. *Applied Surface Science*, 535, 147621. <https://doi.org/10.1016/j.apsusc.2020.147621>
- Yu, J., & Ho, W. (2019). Spinel ferrite photocatalysts: Synthesis, properties, and applications. *Environmental Science: Nano*, 6(10), 3246–3259. <https://doi.org/10.1039/c9en00558b>

11. Said, Z., & Dhaneshwar, R. (2020). Sustainable synthesis and photocatalytic activity of spinel ferrite nanocrystals for wastewater treatment. *Journal of Hazardous Materials*, 385, 121631. <https://doi.org/10.1016/j.jhazmat.2019.121631>

